RESEARCH ARTICLE
doi: 10.2306/scienceasia1513-1874.2024.110

ScienceAsia 50 (6): 2024: ID 2024110: **1–10**

Black rice bran-derived anthocyanins prevent H_2O_2-induced oxidative stress and DNA damage in cholangiocytes through activation of the Nrf2-NQO1 axis

Sasikamon Khophai[a], **Suwadee Chockchaisiri**[b], **Krajang Talabnin**[c], **James R. Ketudat Cairns**[a], **Chutima Talabnin**[a,*]

[a] School of Chemistry, Institute of Science, Suranaree University of Technology, Nakhon Ratchasima 30000 Thailand
[b] College of Allied Health Sciences, Suan Sunandha Rajabhat University, Samut Songkhram 75000 Thailand.
[c] School of Pathology, Institute of Medicine, Suranaree University of Technology, Nakhon Ratchasima 30000 Thailand

*Corresponding author, e-mail: chutima.sub@sut.ac.th

Received 30 Dec 2023, Accepted 3 Aug 2024
Available online 16 Dec 2024

ABSTRACT: Anthocyanins are a group of hydrophilic flavonoids that exhibit various beneficial health effects, including antioxidants and cancer prevention activities. Black rice bran has been demonstrated to be an excellent source of anthocyanins. However, the efficacy of black rice bran-derived anthocyanin has never been demonstrated in cancer prevention for oxidative stress-related cholangiocarcinoma (CCA). In this study, oxidative stress in cholangiocyte cell lines (MMNK-1) was induced by hydrogen peroxide (H_2O_2). The preventive effect of black rice bran-derived anthocyanin (BBR-M-10) in H_2O_2-stimulated cholangiocytes was studied through antioxidant capacity analysis, measurement of intracellular ROS accumulation, and gene expression analysis at both the mRNA and protein levels. Pretreatment with BBR-M-10 decreased oxidative stress in H_2O_2-stimulated MMNK-1 cells by reduction of intracellular ROS accumulation, leading to attenuated oxidative stress-induced cell death in H_2O_2-stimulated MMNK-1 cells, consistent with its up-regulation of survivin and down-regulations of cleaved caspase-3 and cleaved poly (ADP-ribose) polymerase 1 (PARP1). Additionally, BBR-M-10 enhanced the ROS scavenging activity of the endogenous antioxidant system by increasing the transcription level of *Nrf2* and *NQO1* in MMNK-1 cells exposed to H_2O_2. Moreover, BBR-M-10 reduced DNA damage of MMNK-1 cells stimulated by H_2O_2 through down-regulation of phospho-histone H2AX (γH2AX). The cytoprotective properties against oxidative stress suggest their utility in preventing carcinogenic toxicity during CCA development.

KEYWORDS: anthocyanins, oxidative stress, DNA damage, cancer prevention

INTRODUCTION

Oxidative stress is characterized by the overproduction of reactive oxygen species (ROS), which include the superoxide anion (O_2^-), hydrogen peroxide (H_2O_2), and the hydroxyl radical ($OH^\bullet$). These species act as toxic molecules that can damage lipids, proteins, and nucleic acids. Excessive ROS production has been documented in chronic inflammatory-related diseases, including diabetes, neurological diseases, and cancers. A higher ROS level is associated with host-genotoxicity causing DNA base alterations and DNA strand breaks, which result in oncogenic mutation [1, 2]. Additionally, several studies demonstrated that ROS-induced tumorigenesis could occur by a variety of mechanisms: evading the immune response, regulating intracellular signaling, epigenetic changes and genetic instability [2, 3].

Cholangiocarcinoma (CCA) is a highly lethal cancer arising from the epithelial cells of the bile duct. Several risk factors, including choledocholithiasis, Caroli's disease, primary sclerosing cholangitis, cysts, hepatitis B or C virus infection, and liver fluke infections have been linked to chronic inflammation of biliary epithelium and cholangiocarcinogenesis [4]. Chronic inflammation with liver fluke (*Opisthorchis viverrini*: OV) infection is a major cause of oxidative stress-induced CCA development [5]. High levels of oxidized DNA, e.g., 8-oxo-7,8-dihydro-2'-deoxyguanine (8-oxodG) are found in the bile duct epithelial cells of OV-infested hamster liver tissues [6]. Relatedly, a hydrogen peroxide-resistant cholangiocyte cell line presented malignant phenotypes through increased cell growth and the loss of cell-to-cell adhesion [7].

Rice bran, a rice by-product from the milling process, contains a variety of nutrients and bioactive phytochemicals including tocopherols, tocotrienols, oryzanols, vitamins, phenolic acids, and anthocyanins, which exhibit beneficial health effects [8]. Anthocyanins are a group of hydrophilic flavonoids found in pigmented rice including black, red, and brown rice [9, 10]. Interestingly, the highest anthocyanins content is detected in black rice bran, followed by red and brown rice bran [11]. The most abundant anthocyanins in black rice bran are cyanidin-3-glucoside (C3G), peonidin-3-glucoside (P3G), and cyanin 3-O-rutinoside [11]. It has been demonstrated that rice anthocyanins exhibit strong antioxidant activity and display positive effects through anti-inflammation as well as anti-carcinogenesis [12–16]. C3G shows

a preventive effect on the oxidative stress-mediated disease by regulating the nuclear factor erythroid 2 (Nrf2)/antioxidant-responsive element (ARE) pathway [17, 18]. However, the cancer-preventive effect of black rice bran-derived anthocyanins in oxidative stress-related cholangiocarcinoma has never been reported. The current study investigated the preventive effect and underlying mechanism(s) of black rice bran-derived anthocyanins in H_2O_2-stimulation of a cholangiocyte cell line and H_2O_2-induced DNA damage.

MATERIALS AND METHODS

Chemical and reagents

Cyanidin chloride (cat. no. 80022), peonidin chloride (cat. no. 80085), Cyanidin-3-glucoside (cat. no. 89616), and peonidin-3-glucoside (cat. no. 89754) were purchased from PhytoLab GmbH & Co. (Vestenbergsgreuth, Germany). Sulforhodamine B (SRB; cat. no. S1402), TCA (cat. no. T0699), and 2',7'-dichlorodihydrofluorescein diacetate (DCFH-DA; cat. no. D6883) were from Merck (Merck, KGaA, Darmstadt, Germany). TRIzol reagent (cat. no. 15596026), Hoechst 33258 (cat. no. H3569), and the BCA Protein Assay Kit (cat. no. 23225) were obtained from Thermo Fisher Scientific, Inc. (Waltham, MA, USA). SensiFAST cDNA Synthesis Kit (cat. no. BIO-65053) was from Bioline, Meridian (London, UK). LightCycler® 480 SYBR Green I Master mix (cat. no. 04707516001) was from Roche Molecular Systems, Inc. (Pleasanton, CA, USA). Cell culture reagents including DMEM (cat. no. 12100-046), penicillin-streptomycin (cat. no. 15140-122), and fetal bovine serum (cat. no. 10270-098) were from Gibco; Thermo Fisher Scientific, Inc. Primary antibodies against caspase-3 (#9662), cleaved caspase-3 (#9661), survivin (#2808) and gamma H2AX (#80312), and Anti-mouse IgG-Alexa™ 647 conjugate (#4410S) were from Cell Signaling Technology (Danvers, MA, USA). Anti-PARP1 (cat. no. 13371-1) was from Proteintech (Rosemont, IL, USA). Anti β-actin (cat. no. sc-47778) was from Santa Cruz Biotechnology, Inc. (Dallas, TX, USA). HRP-conjugated secondary antibodies (cat. no. NXA931 and NA934), ECL prime blocking reagent (RPN415V), and ECL prime western blot detection (RPN2236) were obtained from Cytiva (Marlborough, MA, USA).

Preparation of black rice bran-derived anthocyanins

Black rice bran from black pigmented rice (*Oryza sativa* L.) was collected from a rice mill, Krabueang Yai, Phimai District, Nakhon Ratchasima Province, Thailand. Black rice bran (5 kg) was soaked with n-hexane followed by 0.1% HCl in methanol (MeOH) at room temperature for 24 h. The MeOH extracts were filtered through filter paper and evaporated in a rotary vacuum evaporator. The powdered extracts (385 g) were subjected to silica column chromatography (CC) using a gradient solvent system of hexane, hexane-ethylacetate (EtOAc), EtOAc, EtOAc-MeOH, and MeOH. Eight fractions (BBR-M-1 to BBR-M-8) were collected, and the anthocyanin contents were investigated by thin-layer chromatography. BBR-M-7 was selected and further purified by Sephadex LH20 CC in MeOH to produce fractions including BBR-M-10, which appeared to have high anthocyanin content. BBR-M-10 was concentrated under reduced pressure. The contents of anthocyanins were further analyzed by thin layer chromatography (TLC) and high-performance liquid chromatography (HPLC).

Thin layer chromatography (TLC)

Cyanidin, peonidin, Cyanidin-3-glucoside, and peonidin-3-glucoside standards and rice bran samples were loaded on pre-coated silica gel plates (5 × 5 cm) (Merck) and developed with a solvent system consisting of *n*-butanol/acetic acid/water, 3:1:1 (v/v). After observing the colored spots, the developed plates were stained by 10% sulfuric acid in methanol, and carbohydrate-containing spots were detected by heating.

High-performance liquid chromatography (HPLC)

Identification of anthocyanin compounds in BBR-M-10 was performed by HPLC on an Agilent Technologies 1260 Infinity HPLC (Agilent Technologies, Santa Clara, CA, USA). Compound separation was performed on a ZORBAX SB-C18 StableBond Analytical 4.6 × 250 mm 3.5-micron column. Mobile phases consisted of 0.1% trifluoroacetic acid (A) and acetonitrile (B) with the following gradient: isocratic 10% B for 5 min, linear increase to 15% B in the following 15 min, isocratic at 15% B for 5 min, then linear increase from 15 to 18% B during the next 5 min and from 18 to 35% B over 20 min. The detection wavelength was 520 nm. The column temperature was set at 35 °C. The flow rate was 1 ml/min, and the injection volume was 20 µl. The peak area was calculated and compared with the cyanidin, peonidin, cyanidin-3-glucoside, and peonidin-3-glucoside standards. A standard curve of individual anthocyanin standards was used to determine the concentration (mg/l) for each anthocyanin compound in BBR-M-10. The amount of total anthocyanin was calculated and expressed as cyanidin-3-glucoside equivalent (CGE) in 100 g the dried powder (dw) as described by Lee et al [19].

Cell culture

The immortalized human cholangiocyte (MMNK-1) cell line was provided by Dr. Sopit Wongkham (Khon Kaen University, Thailand). The certification of authenticity was described by Maruyama et al [20]. MMNK-1 cells were cultured in DMEM supplemented with 10% inactivated fetal bovine serum (FBS), 1%

penicillin-streptomycin, and $NaHCO_3$ in a humidified atmosphere containing 5% CO_2 at 37 °C. The lack of mycoplasma contamination was verified by PCR assay.

Cell viability and compound treatment

MMNK-1 cells were seeded at 7×10^3 cells/well into 96-well plates. After 24 h seeding, the cells were treated with various concentrations of C3G or BBR-M-10 for 24 h. For combination treatment, the cells were pretreated with C3G at 200 µM or BBR-M-10 at 200 or 400 µg/ml for 24 h and then treated with H_2O_2 at 200 µM for another 3 or 6 h at 37 °C in a humidified 5% CO_2 atmosphere. As previously described, a sulforhodamine B (SRB) assay was performed to determine the cell viability [21]. The half-maximum inhibitory concentration (IC_{50}) value was calculated with GraphPad Prism 8 (GraphPad Software, Inc., La Jolla, CA, USA).

Measurement of intracellular ROS accumulation

MMNK-1 cells were seeded at 3.5×10^5 cells per well into 6-well plates and incubated at 37 °C, 5% CO_2 overnight. After 24 h seeding, the cells were pretreated with C3G at 200 µM or BBR-M-10 at 200 or 400 µg/ml for 24 h and then treated with H_2O_2 at 200 µM for another 3 or 6 h at 37 °C in a humidified 5% CO_2 atmosphere. Then, intracellular ROS accumulation was detected with the DCFH-DA fluorescence assay, as previously described [21]. In brief, the cells were stained with 20 mM DCF-DA reagent for 30 min. After a wash with PBS, the stained cells were trypsinized and re-suspended in PBS. The fluorescent signal from DCF-DA was determined in a flow cytometer.

RNA extraction and quantitative RT-PCR

MMNK-1 cells were seeded at 3.5×10^5 cells per well into 6-well plates and incubated at 37 °C, 5% CO_2 overnight. After 24 h seeding, the cells were pretreated with BBR-M-10 at 200 or 400 µg/ml for 24 h and then treated with H_2O_2 at 200 µM for another 1 h at 37 °C in a humidified 5% CO_2 atmosphere. According to the manufacturer's instructions, total RNA was extracted from the MMNK-1 cells with TRIzol reagent. The RNA quality and quantitation were measured by a NanoDrop 2000 spectrophotometer (ThermoFisher Scientific Inc.) and agarose gel electrophoresis. A SensiDAST cDNA Synthesis Kit was used to synthesize cDNA from the RNA. Quantitative PCR using a LightCycler® 480 SYBR Green I Master Mix was performed to investigate the expression level. The primers used for quantitative RT-PCR (Table S1) were described by Talabnin et al [21]. Gene amplification was performed by initial denaturation at 95 °C for 5 min, followed by denaturation at 95 °C for 10 s, annealing at 60 °C for 10 s and extension at 72 °C for 10 s, for 40 cycles. The β-actin gene was used as an internal control. Relative mRNA levels of each gene were normalized with β-actin and calculated by the $2^{-\Delta\Delta CT}$ method [22].

SDS-PAGE and Western blot analysis

Total protein was extracted from MMNK-1 with and without treatment and measured by a BCA assay kit. Thirty micrograms of total proteins from the whole cell lysate of each sample were separated by 10 or 15% SDS-PAGE. The separated proteins were transferred onto nitrocellulose blotting membranes. The nonspecific binding was blocked with 5% ECL prime blocking reagent containing 0.05% Tween 20 at room temperature for 1 h. Then, the membranes were incubated at 4 °C overnight with primary antibody at dilutions of 1:1,000 for caspase-3, cleaved caspase-3, survivin, and γH2AX; 1:2,000 for β-actin; or 1:5,000 for PARP1 in PBS containing 0.05% Tween 20 (PBST). After that, the membranes were washed with PBST and incubated with HRP-conjugated secondary antibody at a dilution of 1:2,000 for 1 h at room temperature. Finally, the target proteins were detected and visualized by ECL prime western blot detection. The signal density of each target protein was determined with Image J software (version 1.53a; National Institutes of Health) and normalized to β-actin.

Antioxidant capacity analysis

Measurement of antioxidant capacity was performed through 2,2'-diphenyl-1-picrylhydrazyl radical (DPPH) and 2,2'-azino-bis (3-ethylbenzthiazoline-6-sulphonic acid) (ABTS) assays. Ascorbic acid was used as the antioxidant standard.

The DPPH assay was performed as described by Brand-Williams et al [23]. Various concentrations of BBR-M-10 (0–800 µg/ml) and ascorbic acid standard (0–800 µg/ml) were prepared in 100% (v/v) methanol. Then, 10 µl of sample or standards were mixed with 190 µl of 0.1 mM $DPPH^{\bullet}$ solution and incubated for 30 min in the dark. The absorbance at 517 nm was measured in a microplate reader. The percentage of DPPH radical scavenging activity was calculated by the following equation: DPPH radical scavenging activity (%) $= [(A_0 - A_1)/A_0] \times 100$; where A_0 is the absorbance of the control, and A_1 is the absorbance of the sample.

The ABTS assay was performed as previously described by Van den Berg et al [24]. Various concentrations of BBR-M-10 (0–800 µg/ml) and ascorbic acid standard (0-800 µg/ml) were prepared in 100% methanol. Then, 20 µl of sample or standards were mixed with 180 µl of 7.0 mM $ABTS^{\bullet+}$ solution and incubated for 30 min at room temperature. The decrease of absorbance was measured in a microplate reader at 734 nm. The percentage of ABTS radical scavenging activity was calculated by the following equation: ABTS radical scavenging activity (%) $= [(A_0 - A_1)/A_0] \times 100$; where A_0 is the absorbance of

the control, and A_1 is the absorbance of the sample.

The IC_{50} values for DPPH or ABTS radical scavenging activities were calculated in GraphPad Prism 8 (GraphPad Software, Inc.).

Immunofluorescent analysis

MMNK-1 cells were seeded at 4×10^4 cells per well into 8-well cell culture slides and incubated at 37 °C, 5% CO_2 overnight. After 24 h seeding, the cells were pretreated with BBR-M-10 at 200 or 400 µg/ml for 24 h and then treated with H_2O_2 at 200 µM for another 3 h at 37 °C in a humidified 5% CO_2 atmosphere. Then, the cells were washed by PBS and fixed with 4% paraformaldehyde. The fixed cells were permeabilized with 0.1% Triton-X100 in PBS for 10 min on ice. Blocking solution (2% bovine serum albumin in 0.1% PBST) was added into the cells for 30 min on ice, and then the cells were incubated at 4 °C overnight with anti-γ-H2AX (1:100). After washing with PBS, Alexa™ 647 conjugated anti-mouse IgG (1:500) was used as secondary antibodies and incubated for 30 min in a dark area. Nuclear counterstain with Hoechst 33258 solution (1:1,000) was applied for 10 min. The stained cells were visualized on a confocal microscope (Carl Zeiss, Oberkochen, Germany).

Statistical analysis

All data points are expressed as the mean ± standard deviation (SD) of 3 replicated experiments. GraphPad Prism software (version 8.0; GraphPad Software, Inc., USA) was used for statistical analysis. The student-*t* test was applied to calculate the significance of differences between groups. Differences were considered statistically significant when the *p*-values were less than 0.05.

RESULTS

Cyanidin-3-glucoside is a major anthocyanin composition in black rice bran extract (BBR-M-10)

Upon fractionation of black rice bran extract, the fraction that appeared to contain the highest concentration of anthocyanins based on coloration was designated BBR-M-10. Total anthocyanin content in BBR-M-10 was 108 mg CGE/100 g dw (100.37 mg/l). Then, BBR-M-10 was analyzed by TLC and HPLC techniques to determine its anthocyanin composition. TLC analysis suggested that the main anthocyanin components in BBR-M-10 were cyanidin-3-glucoside (C3G) and peonidin-3-glucoside (P3G) (Fig. 1a). This result was consistent with HPLC analysis, in which C3G was found in BBR-M-10 in the highest amount of 94.54 mg/l whereas P3G and cyanidin concentrations were 7.28 and 2.47 mg/l, respectively (Fig. 1b). Next, DPPH and ABTS assays demonstrated that the radical scavenging activity of BBR-M-10 was increased in a dose-dependent manner. At a concentration of 400 µg/ml, the radical scavenging activities in the DPPH and ABTS assay of BBR-M-10 were 80.7 ± 1.2% and 79.3 ± 1.2%, respectively, whereas at the same concentration, the radical scavenging activities of ascorbic acid standard were 86.5 ± 0.9% for DPPH and 92.3 ± 1.7% for ABTS. Additionally, the IC_{50} values in the DPPH and ABTS assays for BBR-M-10 were 128 and 100 µg/ml, respectively, whereas IC_{50} values of ascorbic acid in the DPPH and ABTS assays were 90.8 and 66.0 µg/ml, respectively (Fig. 1c,d). These results show that the antioxidant capacity of BBR-M-10 is comparable with that of ascorbic acid.

BBR-M-10 attenuates oxidative stress-induced cell death in H_2O_2-stimulated cholangiocyte cells

In this study, an H_2O_2-stimulated cholangiocyte (MMNK-1) model was used to investigate the effect of BBR-M-10 on cancer prevention. Firstly, the cytotoxic effect of BBR-M-10 on MMNK-1 cells was determined. MMNK-1 cells were treated with BBR-M-10 at various concentrations (0–1,250 µg/ml) and incubated for 24 h. A cytotoxic effect of BBR-M-10 was observed at the concentration more than 312.5 µg/ml, but the IC_{50} value for MMNK-1 was 753 µg/ml (Fig. 2a). Therefore, BBR-M-10 concentrations at 200 and 400 µg/ml were selected to use in subsequent experiments since those concentrations are considered as non-cytotoxic, evidenced by percentage of cell viability above 80%.

Then, the effect of H_2O_2 on MMNK-1 cell viability was also examined. MMNK-1 cells were treated with H_2O_2 at various concentrations (0–1,000 µM) and incubated for 6 h. Cell viability decreased in a dose-dependent manner, and the IC_{50} value was 155 µM (Fig. 2b). As a result, H_2O_2 at 200 µM was used to induce oxidative stress in MMNK-1 cholangiocytes. Next, cell viability was used to investigate whether BBR-M-10 attenuates oxidative stress-induced cell death in H_2O_2-stimulated MMNK-1 cells. Pretreatment with BBR-M-10 at 200 and 400 µg/ml for 24 h enhanced the viability of MMNK-1 cells stimulated by H_2O_2 (Fig. 2c). Similar preventive effects were also observed in H_2O_2-stimulated MMNK-1 cells with C3G pretreatment (Fig. 2d). Furthermore, western blot analysis demonstrated that up-regulation of survivin and down-regulation of cleaved caspase-3 and cleaved PARP1 were clearly observed in H_2O_2-stimulated MMNK-1 cells with BBR-M-10 pretreatment (Fig. 2e). These findings indicate that C3G in BBR-M-10 may play a role in decreasing the toxic effect of H_2O_2 on MMNK-1 cells.

BBR-M-10 alleviates oxidative stress in H_2O_2-stimulated cholangiocyte cells by reducing ROS accumulation and up-regulation of *NQO1*

The intracellular ROS accumulation and expression of phase II antioxidant genes were measured to investigate the mechanism of BBR-M-10 reduction of oxidative stress in H_2O_2-stimulated MMNK-1 cells. The intracellular ROS accumulation was evaluated

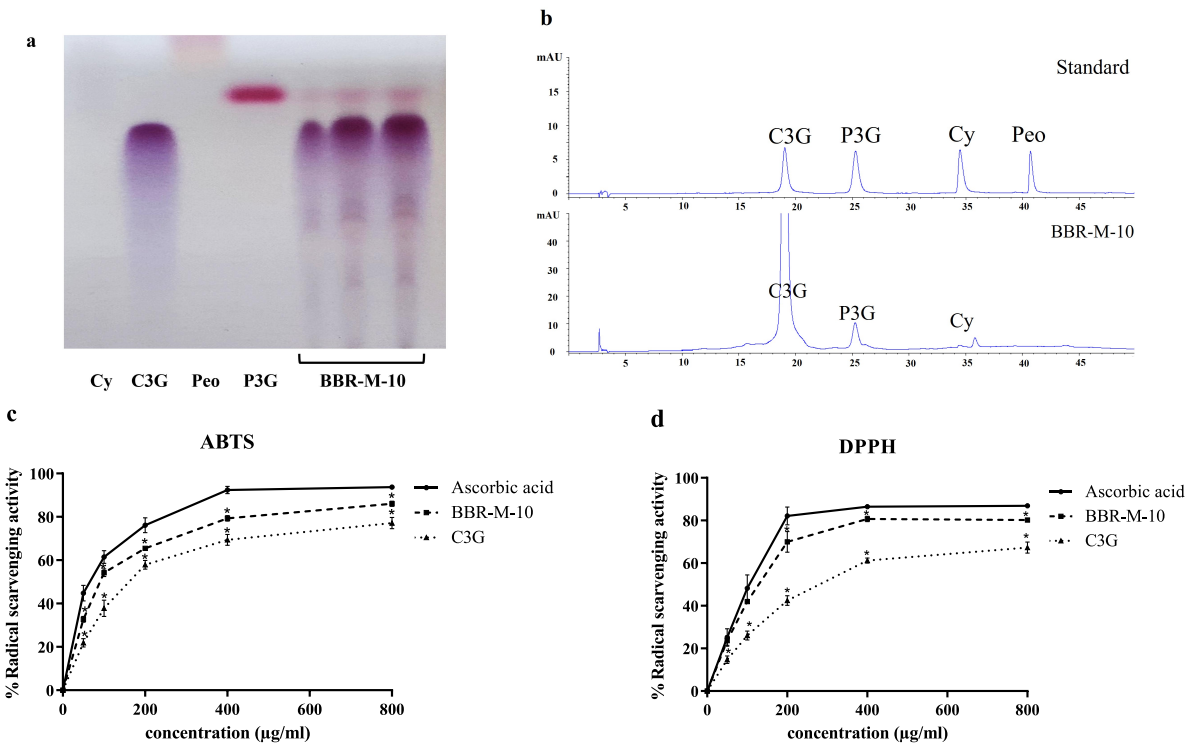

Fig. 1 Identification and quantitative analysis of anthocyanin composition in black rice bran extract (BBR-M-10) and their antioxidant capacity. (a) Thin layer chromatography of BBR-M-10 and standard anthocyanins including cyanidin (Cy), cyanidin-3-glucoside (C3G), peonidin (Peo), and peonidin-3-glucoside (P3G). (b) High-performance liquid chromatography of BBR-M-10. (c and d) Antioxidant activity of BBR-M-10 in ABTS and DPPH assays. Values are expressed as mean ± standard deviation of 3 independent experiments. * $p < 0.05$ versus ascorbic acid; $p < 0.05$ was defined as statistically significant.

by DCF-DA staining and analyzed by flow cytometry. H_2O_2 induced intracellular ROS accumulation in a time-dependent manner. However, pretreatment with BBR-M-10 or C3G significantly decreased intracellular ROS accumulation in H_2O_2-stimulated MMNK-1 cells at 3 and 6 h (Fig. 3a,b). Next, the expression levels of 8 phase II antioxidant genes were investigated by quantitative RT-PCR. The result showed that mRNA expression levels of phase II antioxidant genes, including Nuclear Factor Erythroid-2-Related Factor 2 (*Nrf2*), glutamate-cysteine ligase modifier subunit (*GCLM*), NAD(P)H quinone dehydrogenase 1 (*NQO1*), glutathione S-transferase P (*GSTP-1*), and superoxide dismutase 2 (*SOD2*) were significantly increased in BBR-M-10 treated MMNK-1 compared with those of control cells (Fig. 3c). Moreover, *NQO1* was most highly expressed in BBR-M-10 treated MMNK-1 cells among all phase II antioxidant genes (Fig. 3c). As a result, the mRNA expression levels of *Nrf2* and *NQO1* were determined to investigate whether BBR-M-10 diminishes ROS accumulation in H_2O_2-stimulated MMNK-1 cells by activating the Nrf2 pathway. The mRNA expression levels of *Nrf2* and *NQO1* were significantly increased in H_2O_2-stimulated MMNK-1 cells with BBR-M-10 pretreatment (Fig. 3d,e). These findings suggest that BBR-M-10 has an antioxidant effect through activation of the Nrf2-NQO1 axis.

BBR-M-10 reduces H_2O_2-induced DNA damage in cholangiocyte cells

To evaluate the preventive effect of BBR-M-10 against oxidative stress-induced DNA damage, γH2AX, a marker for DNA double-strand breaks (DSBs), was examined in H_2O_2-stimulated MMNK-1 cells with or without BBR-M-10 pretreatment. Immunofluorescent analysis showed that γH2AX levels increased in H_2O_2-stimulated MMNK-1 cells. Nevertheless, pretreatment with BBR-M-10 at 200 and 400 µg/ml for 24 h decreased the γH2AX signal, suggesting that BBR-M-10 reduced DNA damage of MMNK-1 cells stimulated by H_2O_2 (Fig. 4a). Moreover, western blot analysis confirmed that BBR-M-10 pretreatment decreased γH2AX in H_2O_2-stimulated MMNK-1 cells (Fig. 4b). These results show that BBR-M-10 possesses cytoprotective properties against oxidative stress through the reduction of ROS accumulation and DNA damage in MMNK-1.

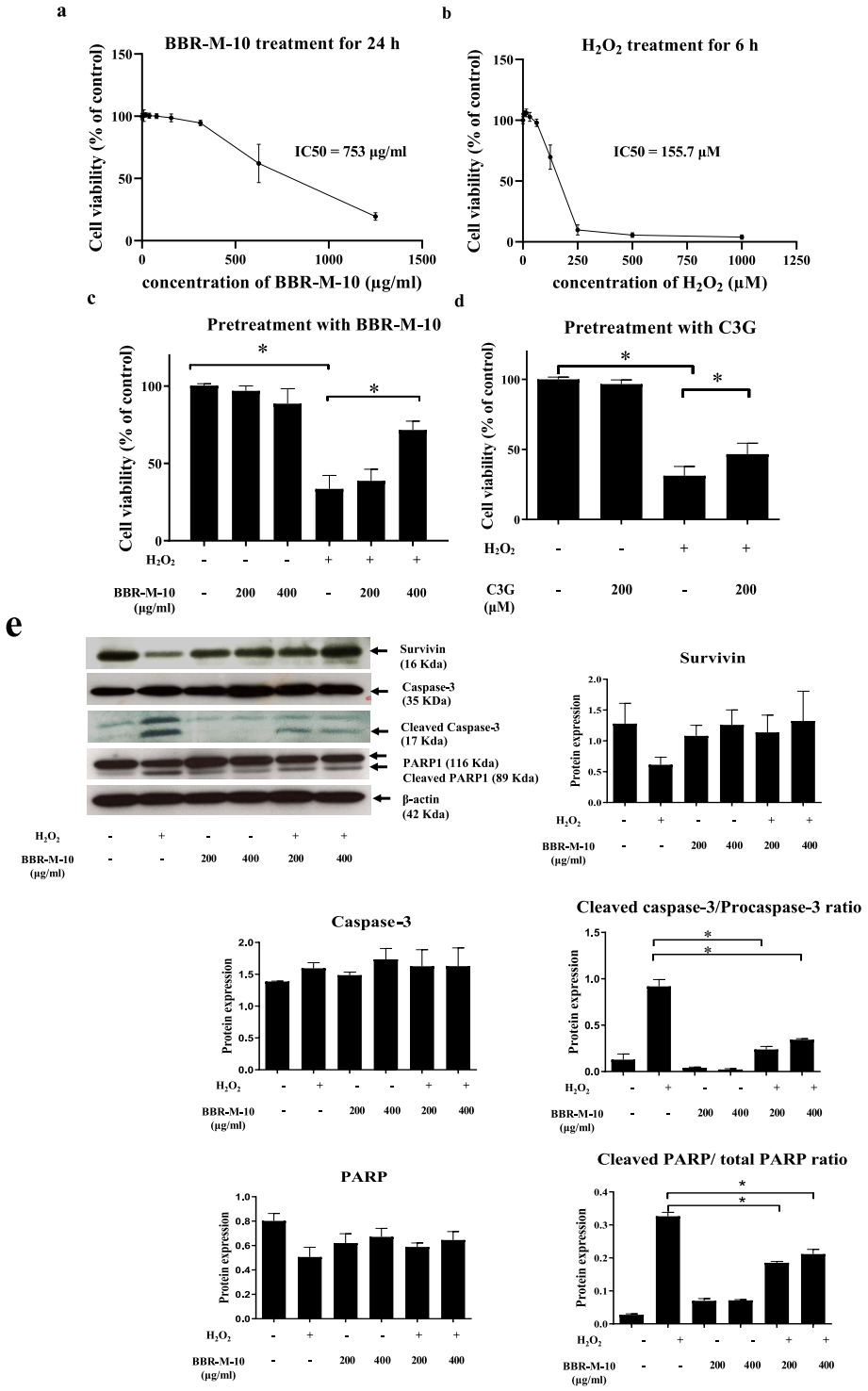

Fig. 2 Effect of BBR-M-10 on oxidative stress-induced cell death. (a) Cytotoxic effect of BBR-M-10 in MMNK-1 cells treated for 24 h and (b) cytotoxic effect of H_2O_2 in MMNK-1 cells treated for 6 h determined by SRB assay. Cell viability of H_2O_2-stimulated MMNK-1 cells with pretreatment with BBR-M-10 (c) or C3G (d) for 24 h. (e) The protein expression of apoptotic proteins (caspase-3, cleaved caspase-3, and PARP1) and survivin determined in H_2O_2-stimulated MMNK-1 cells with pretreatment with BBR-M-10 and control cells by Western blot analysis. Representative data from 3 independent experiments are shown. Values are presented as mean ± standard deviation. *, $p < 0.05$ versus H_2O_2-stimulated MMNK-1 without pretreatment which was defined as statistically significant.

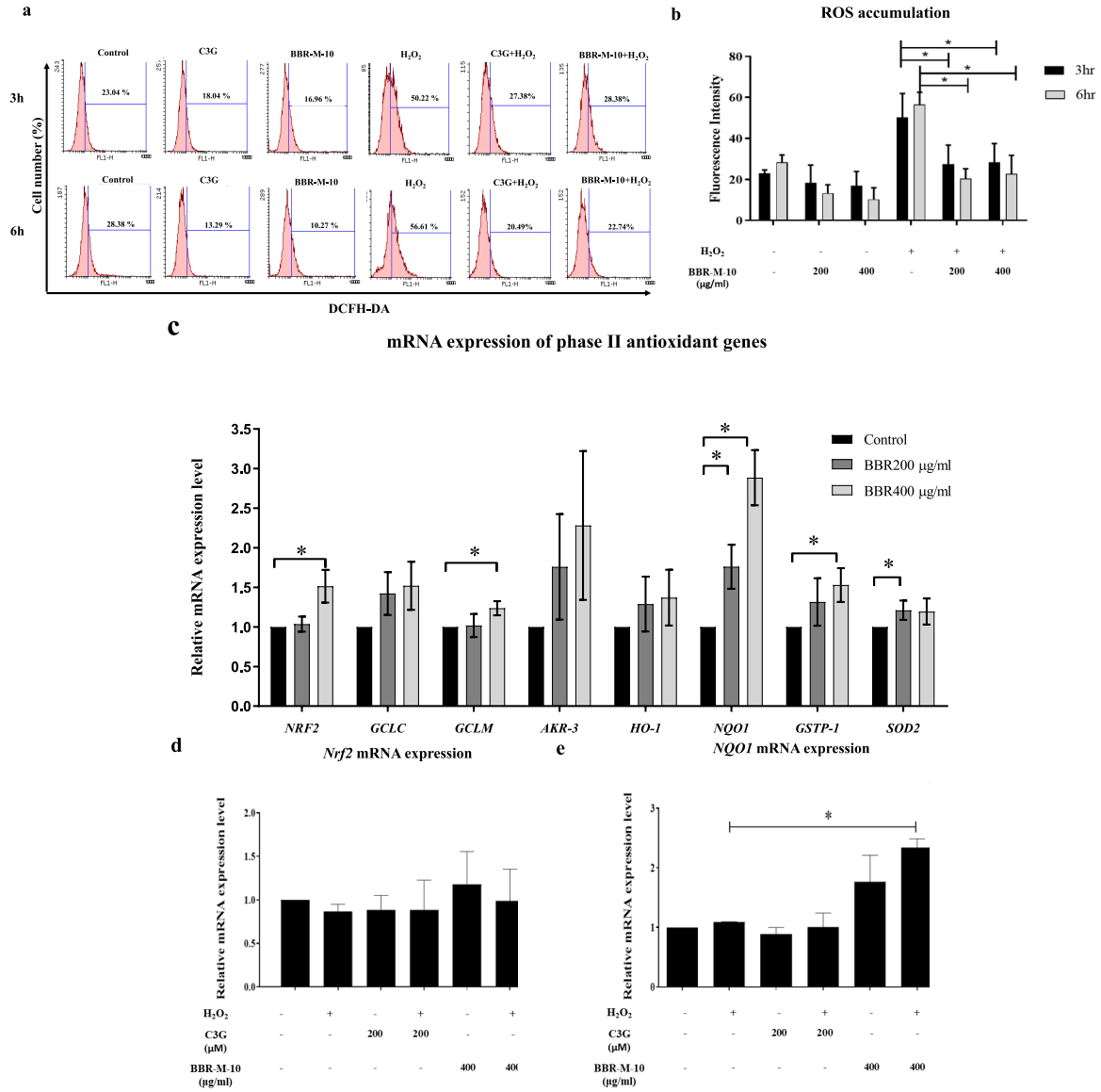

Fig. 3 BBR-M-10 promoting antioxidant activity through the Nrf2-NQO1 axis. (a and b) ROS accumulation of H_2O_2-stimulated MMNK-1 cells pretreated with BBR-M-10 for 3 and 6 h. (c) mRNA expressions of 8 phase II antioxidant genes determined in BBR-M-10 treated MMNK-1 cells and control cells by quantitative RT-PCR. The respective mRNA expression of *Nrf2* (d) and *NQO1* (e) investigated in H_2O_2-stimulated MMNK-1 with pretreatment of BBR-M-10 or C3G and control cells. Values are presented as mean ± standard deviation of 3 independent experiments. *, $p < 0.05$ versus H_2O_2-stimulated MMNK-1 without pretreatment which was defined as statistically significant.

DISCUSSION

Pigmented rice is a functional food high in phytochemicals such as polyphenols and anthocyanins. Anthocyanins are mainly found in pigmented rice bran, which consists of 2 major components including the pericarp and aleurone layers of the grains. The highest anthocyanin content is observed in black rice bran compared to red and brown rice bran [25]. Anthocyanins exhibit several biological activities, including antioxidants, anti-cancer, anti-apoptosis, and anti-inflammation. [18, 26]. In the present study, we demonstrated that black rice bran extract (BBR-M-10) contained C3G as the major anthocyanin and had a high antioxidant capacity associated with a decrease in oxidative stress-induced cell death and DNA damage in H_2O_2-stimulated cholangiocyte cells.

Overproduction of reactive oxygen species (ROS)

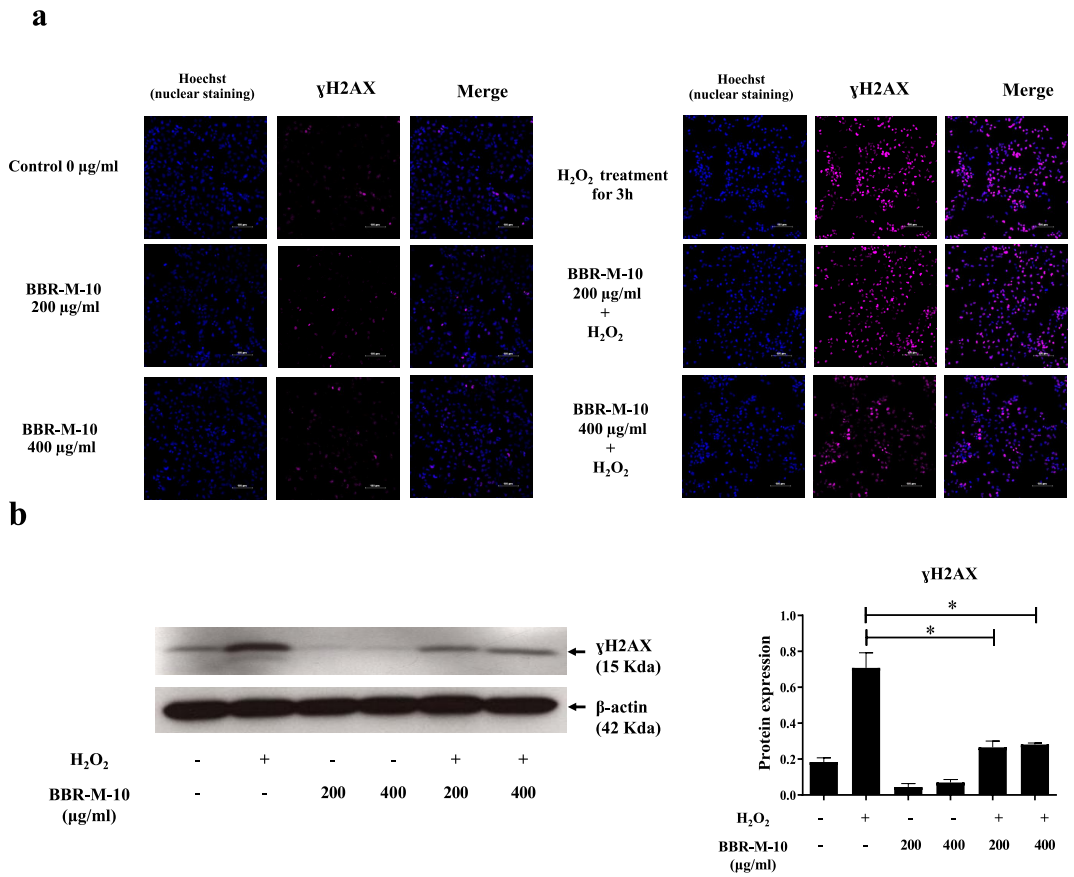

Fig. 4 Effect of BBR-M-10 on oxidative stress-induced DNA damage. MMNK-1 cells were pretreated with BBR-M-10 and then treated with H_2O_2 at 200 μM for another 3 h. The expression of DNA damage response (γ-H2AX) observed by immunofluorescent staining ((a); ×200 magnification, scale bar, 100 μm) and Western blot analysis (b). The stained cells were visualized on a confocal microscope (Carl Zeiss). Representative data from 3 independent experiments are shown. Values are presented as mean ± standard deviation. *, $p < 0.05$ versus H_2O_2-stimulated MMNK-1 without pretreatment. p<0.05 was defined as statistically significant.

and reactive nitrogen species (RNS) is a major cause of cholangiocarcinoma development due to long-term exposure to inflammation from liver fluke infection (*O. viverrini*). Additionally, chronic treatment of cholangiocytes with H_2O_2 has demonstrated that the cells can adapt to oxidative stress and demonstrate malignant phenotypes such as the increase of cell growth and the loss of cell-to-cell adhesion [7]. As a result, high levels of etheno-DNA adducts, 8-nitroguanine, and 8-oxodG, are formed during CCA development [6, 28]. Many studies have shown that anthocyanins, especially C3G, modulate oxidative stress against DNA damage and apoptosis [18]. In the present study, the pretreatment with BBR-M-10 significantly decreased intracellular ROS accumulation in H_2O_2-stimulated MMNK-1 cells, leading to enhanced viability of the MMNK-1cells. This could be due to their chemical structure, especially the 3′ and 4′ hydroxyl groups on the B-ring which are the active site for scavenging free radicals, thereby decreasing the intracellular ROS accumulation in H_2O_2-stimulated cholangiocyte cells.

Several studies demonstrated that C3G modulates oxidative stress through the nuclear factor erythroid 2-related factor 2 (Nrf2)/antioxidant-responsive element (ARE) pathway [18]. A similar observation was made for BBR-M-10, since *Nrf2*, *GCLM*, *NQO1*, *GSTP-1*, and *SOD2* were highly expressed in BBR-M-10 treated MMNK-1 cells. Furthermore, mRNA expression of *Nrf2* and *NQO1* was significantly increased in H_2O_2-stimulated MMNK-1 cells with BBR-M-10 pretreatment. The results of the present study suggest that C3G in BBR-M-10 regulates the transcriptional levels of *Nrf2* target genes to reduce ROS accumulation in H_2O_2-stimulated MMNK-1 cells. These findings agree with the studies on H_2O_2-treated HepG2 cells and glutamate-treated HT22 hippocampal neuronal cells,

in which pretreatment with C3G protects against cell death from ROS-mediated stress through the increased expression of *Nrf2* and *Nrf2*-target genes such as *HO* and *NQO1* [29, 30]. Moreover, chronic inflammation-mediated DNA lesions have been demonstrated in liver fluke-induced cholangiocarcinoma through the formation of high levels of 8-oxodG [6, 28]. Excessive amounts of ROS form the 8-oxodG, and a high level of 8-oxodG in CCA tissues is associated with poor prognosis [31]. Additionally, high levels of 8-oxodG are detected in cancer stem-like cells of CCA (CD133 and Oct3/4-positive cells) and associated with high expression of DNA damage response (indicated by the presence of γ-H2AX) [32]. In the present study, γH2AX expression was increased in H_2O_2-stimulated MMNK-1 cells. Pretreatment with BBR-M-10 in MMNK-1 cells stimulated by H_2O_2 reduced γH2AX expression. These observations suggest that BBR-M-10 exhibits cytoprotective properties against oxidative stress through the reduction of ROS accumulation, leading to a decrease in DNA damage in MMNK-1 cells. However, further studies on 8-oxodG formation will be required to support the utility of BRR-M-10 in CCA prevention. Verification of the preventive effect of BBR-M-10 *in vivo* will be examined further.

CONCLUSION

Pretreatment of black rice bran-derived anthocyanins (BBR-M-10) protected MMNK-1 cells from H_2O_2-induced oxidative stress and DNA damage. Pretreatment with BBR-M-10 decreased ROS accumulation through the increased transcription of *Nrf2* and *NQO1* in MMNK-1 cells exposed to H_2O_2. Taken together, our findings suggest the utility of black rice bran-derived anthocyanins in preventing carcinogenic toxicity during CCA development.

Appendix A. Supplementary data

Supplementary data associated with this article can be found at https://dx.doi.org/10.2306/scienceasia1513-1874.2024.110.

Acknowledgements: This work was supported by the Thailand Research Fund international research network grant IRN62W0004 and the Suranaree University of Technology, Thailand Science Research and Innovation (TSRI), and National Science, Research, and Innovation Fund (NSRF) (NRIIS number 160335). We thank Mr. Bryan Roderick Hamman for assistance with the English-language presentation of the manuscript.

REFERENCES

1. Hayes JD, Dinkova-Kostova AT, Tew KD (2020) Oxidative stress in cancer. *Cancer Cell* **38**, 167–197.
2. Arfin S, Jha NK, Jha SK, Kesari KK, Ruokolainen J, Roychoudhury S, Rathi B, Kumar D (2021) Oxidative stress in cancer cell metabolism. *Antioxidants (Basel)* **10**, 642–642.
3. Liou GY, Storz P (2010) Reactive oxygen species in cancer. *Free Radical Res* **44**, 479–496.
4. Banales JM, Marin JJG, Lamarca A, Rodrigues PM, Khan SA, Roberts LR, Cardinale V, Carpino G, et al (2020) Cholangiocarcinoma 2020: the next horizon in mechanisms and management. *Nat Rev Gastroenterol Hepatol* **17**, 557–588.
5. Sripa B, Kaewkes S, Sithithaworn P, Mairiang E, Laha T, Smout M, Pairojkul C, Bhudhisawasdi V, et al (2007) Liver fluke induces cholangiocarcinoma. *PLoS Med* **4**, e201.
6. Pinlaor S, Ma N, Hiraku Y, Yongvanit P, Semba R, Oikawa S, Murata M, Sripa B, et al (2004) Repeated infection with *Opisthorchis viverrini* induces accumulation of 8-nitroguanine and 8-oxo-7,8-dihydro-2′-deoxyguanine in the bile duct of hamsters via inducible nitric oxide synthase. *Carcinogenesis* **25**, 1535–1542.
7. Thanan R, Techasen A, Hou B, Jamnongkan W, Armartmuntree N, Yongvanit P, Murata M (2015) Development and characterization of a hydrogen peroxide-resistant cholangiocyte cell line: A novel model of oxidative stress-related cholangiocarcinoma genesis. *Biochem Biophys Res Commun* **464**, 182–188.
8. Pitija K, Muntana N, Sriseadka T, Vanavichit A, Mahatheeranont S (2013) Anthocyanin content and antioxidant capacity in bran extracts of some Thai black rice varieties. *Int J Food Sci Technol* **48**, 300–308.
9. Francavilla A, Joye IJ (2020) Anthocyanins in whole grain cereals and their potential effect on health. *Nutrients* **12**, 2922–2942.
10. Yamuangmorn S, Prom UTC (2021) The potential of high-anthocyanin purple rice as a functional ingredient in human health. *Antioxidants (Basel)* **10**, 833–854.
11. Karimi E, Mehrabanjoubani P, Keshavarzian M, Oskoueian E, Jaafar HZ, Abdolzadeh A (2014) Identification and quantification of phenolic and flavonoid components in straw and seed husk of some rice varieties (*Oryza sativa* L.) and their antioxidant properties. *J Sci Food Agric* **94**, 2324–2330.
12. Yamsaray M, Sreewongchai T, Phumichai C, Chalermchaiwat P (2023) Yield and nutritional properties of improved red pericarp Thai rice varieties. *ScienceAsia* **49**, 155–160.
13. Zheng HX, Qi SS, He J, Hu CY, Han H, Jiang H, Li XS (2020) Cyanidin-3-glucoside from black rice ameliorates diabetic nephropathy via reducing blood glucose, suppressing oxidative stress and inflammation, and regulating transforming growth factor beta1/Smad expression. *J Agric Food Chem* **68**, 4399–4410.
14. Semmarath W, Mapoung S, Umsumarng S, Arjsri P, Srisawad K, Thippraphan P, Yodkeeree S, Dejkriengkraikul P (2022) Cyanidin-3-O-glucoside and peonidin-3-O-glucoside-Rich fraction of black rice germ and bran suppresses inflammatory responses from SARS-CoV-2 spike glycoprotein S1-induction *in vitro* in A549 lung cells and THP-1 macrophages via inhibition of the NLRP3 inflammasome pathway. *Nutrients* **14**, 2738–2760.
15. Punvittayagul C, Chariyakornkul A, Sankam P, Wongpoomchai R (2021) Inhibitory effect of Thai purple rice husk extract on chemically induced carcinogenesis in rats. *Molecules* **26**, 360–372.
16. Guo H, Punvittayagul C, Vachiraarunwong A, Phannasorn W, Wongpoomchai R (2022) Cancer chemopreventive potential of cooked glutinous purple rice on the early stages of hepatocarcinogenesis in rats. *Front Nutr*

9, 1032771.
17. Nantacharoen W, Baek SJ, Plaingam W, Charoenkiatkul S, Tencomnao T, Sukprasansap M (2022) *Cleistocalyx nervosum* var. *paniala* berry promotes antioxidant response and suppresses glutamate-induced cell death via SIRT1/Nrf2 survival pathway in hippocampal HT22 neuronal cells. *Molecules* **27**, 5813–5834.
18. Rahman S, Mathew S, Nair P, Ramadan WS, Vazhappilly CG (2021) Health benefits of cyanidin-3-glucoside as a potent modulator of Nrf2-mediated oxidative stress. *Inflammopharmacology* **29**, 907–923.
19. Lee SG, Vance TM, Nam T-G, Kim D-O, Koo SI, Chun OK (2016) Evaluation of pH differential and HPLC methods expressed as cyanidin-3-glucoside equivalent for measuring the total anthocyanin contents of berries. *J Food Meas Charact* **10**, 562–568.
20. Maruyama M, Kobayashi N, Westerman KA, Sakaguchi M, Allain JE, Totsugawa T, Okitsu T, Fukazawa T, et al (2004) Establishment of a highly differentiated immortalized human cholangiocyte cell line with SV40T and hTERT. *Transplantation* **77**, 446–451.
21. Talabnin C, Talabnin K, Wongkham S (2020) Enhancement of piperlongumine chemosensitivity by silencing heme oxygenase-1 expression in cholangiocarcinoma cell lines. *Oncol Lett* **20**, 2483–2492.
22. Livak KJ, Schmittgen TD (2001) Analysis of relative gene expression data using real-time quantitative PCR and the $2^{-\Delta\Delta C_T}0$ method. *Methods* **25**, 402–408.
23. Brand-Williams W, Cuvelier ME, Berset C (1995) Use of a free radical method to evaluate antioxidant activity. *LWT Food Sci Technol* **28**, 25–30.
24. van den Berg R, Haenen GRMM, van den Berg H, Bast A (1999) Applicability of an improved Trolox equivalent antioxidant capacity (TEAC) assay for evaluation of antioxidant capacity measurements of mixtures. *Food Chem* **66**, 511–517.
25. Shao Y, Xu F, Sun X, Bao J, Beta T (2014) Identification and quantification of phenolic acids and anthocyanins as antioxidants in bran, embryo and endosperm of white, red and black rice kernels (*Oryza sativa* L.). *J Cereal Sci* **59**, 211–218.
26. Olivas-Aguirre FJ, Rodrigo-Garcia J, Martinez-Ruiz ND, Cardenas-Robles AI, Mendoza-Diaz SO, Alvarez-Parrilla E, Gonzalez-Aguilar GA, de la Rosa LA, et al (2016) Cyanidin-3-O-glucoside: Physical-chemistry, foodomics and health effects. *Molecules* **21**, 1264–1294.
27. Sripa B, Pairojkul C (2008) Cholangiocarcinoma: lessons from Thailand. *Curr Opin Gastroen* **24**, 349–356.
28. Dechakhamphu S, Yongvanit P, Nair J, Pinlaor S, Sithithaworn P, Bartsch H (2008) High excretion of etheno adducts in liver fluke-infected patients: protection by praziquantel against DNA damage. *Cancer Epidemiol Biomarkers Prev* **17**, 1658–1664.
29. Yu L, Zhang S-d, Zhao X-l, Ni H-y, Song X-r, Wang W, Yao L-p, Zhao X-h, et al (2020) Cyanidin-3-glucoside protects liver from oxidative damage through AMPK/Nrf2 mediated signaling pathway *in vivo* and *in vitro*. *J Funct Foods* **73**, 104148.
30. Sukprasansap M, Chanvorachote P, Tencomnao T (2020) Cyanidin-3-glucoside activates Nrf2-antioxidant response element and protects against glutamate-induced oxidative and endoplasmic reticulum stress in HT22 hippocampal neuronal cells. *BMC Complementary Med Ther* **20**, 46–58.
31. Thanan R, Oikawa S, Hiraku Y, Ohnishi S, Ma N, Pinlaor S, Yongvanit P, Kawanishi S, et al (2014) Oxidative stress and its significant roles in neurodegenerative diseases and cancer. *Int J Mol Sci* **16**, 193–217.
32. Thanan R, Pairojkul C, Pinlaor S, Khuntikeo N, Wongkham C, Sripa B, Ma N, Vaeteewoottacharn K, et al (2013) Inflammation-related DNA damage and expression of CD133 and Oct3/4 in cholangiocarcinoma patients with poor prognosis. *Free Radical Biol Med* **65**, 1464–1472.

Appendix A. Supplementary data

Table S1 Primers used for quantitative RT-PCR.

Gene	5′-Forward-3′	5′-Reverse-3′
Nrf2	5′-TACTCCCAGGTTGCCCACA-3′	5′-CATCTACAAACGGGAATGTCTGC-3′
GCLC	5′-ATGCCATGGGATTTGGAAT-3′	5′-AGATATACTGCAGGCTTGGAATG-3′
GCLM	5′-GACAAAACACAGTTGGAACAGC-3′	5′-CAGTCAAATCTGGTGGCATC-3′
AKR1C3	5′-CATTGGGGTGTCAAACTTCA-3′	5′-CCGGTTGAAATACGGATGAC-3′
HMOX1	5′-CAACATCCAGCTCTTTGAGGA-3′	5′-GGGCAGAATCTTGCACTTTG-3′
NQO1	5′-GATATTCCAGTTCCCCCTGC-3′	5′-TTCTTACTCCGGAAGGGTCC-3′
GSTP1	5′-TACACCAACTATGAGGCGGG-3′	5′-AGCGAAGGAGATCTGGTCTC-3′
SOD2	5′-GTTGGCCAAGGGAGATGTTAC-3′	5′-AGCAACTCCCCTTTGGGTTC-3′
B-actin	5′-GATCAGCAAGCAGGAGTATGACG-3′	5′-AAGGGTGTAACGCAACTAAGTCATAG-3′

Nrf2, nuclear factor erythroid 2-related factor 2; *GCLM*, γ-glutamylcysteine synthetase modifier subunit; *GCLC*, γ-glutamylcysteine synthetase catalytic subunit; *AKR1C3*, aldo-keto reductase 1 subunits C-3; *HO-1*, heme oxygenase-1; *NQO1*, NADPH quinone oxidoreductase-1; *GSTP1*, glutathione S-transferase P1; and *SOD2*, superoxide dismutase 2.